Sparse Deconvolution and Causality Analysis of Inflammatory Markers During Cardiac Surgery

Vidya Raju, *Member, IEEE*, Ben Gibbison, Behnam Hajihossainlou, Elizabeth B. Klerman and Rose T. Faghih, *Senior Member, IEEE*

Abstract—Major bodily trauma such as cardiac surgery elicits (in response to tissue injury and other exogenous surgical factors) a whole-body inflammation response during which specialized signaling proteins called cytokines are synthesized and invoke multiple defense mechanisms. Many proinflammatory and anti-inflammatory cytokines such as interleukins (IL) and tumor necrosis factor (TNF) are produced to initiate bodily repair. Due to the adverse health consequences, including mortality, of a maladaptive cytokine response, understanding their complex dynamics using system-theoretic modeling and analysis may pave the way for controlling the inflammatory response which may eventually improve medical outcomes for patients. To this end, we use clinical data from ten patients undergoing coronary arterial bypass graft surgery to study the response of four cytokines (IL6, IL8, IL10, TNF α) and the neuroendocrine hormone cortisol. We perform deconvolution to obtain the secretory pulses underlying their pulsatile production and analyze causal interactions, mathematically uncovering some interactive relationships found in previous experimental studies.

Clinical relevance— This work is a first step towards a mechanistic inference of the inflammatory response to surgery that could eventually help control the inflammatory response and could inform medical interventions to improve patient outcomes.

I. INTRODUCTION

When the body is disturbed from its systemic equilibrium (e.g., due to bacterial or viral infections, injury or surgery), the immune system initiates the production of proteins called cytokines that play a crucial role in signaling the disturbance to the brain and other cells, so that other physiological responses can occur to restore the body to a healthy state [1], [2]. For instance, injury due to small tissue wounds results in the local inflammation response, during which the cytokines signal the presence of injury, regulate the transport of extracellular matter such as collagen, alter the proliferation

The work was supported in part by NSF under Grant 2226123 - CAREER: MINDWATCH: Multimodal Intelligent Noninvasive brain state Decoder for Wearable AdapTive Closed-loop arcHitectures and in part by NYU start-up funds. R. T. Faghih served as the senior author.

V. Raju and R. T. Faghih are with the Department of Biomedical Engineering, Tandon School of Engineering, New York University, 10012 {vidya.raju,rfaghih}@nyu.edu

B. Gibbison is with the Department of Anaesthesia, University of Bristol, UK and University Hospitals Bristol NHS Foundation Trust, Bristol BS2 8HW, UK. ben.gibbison@bristol.ac.uk

Behnam Hajihossainlou is with the Department of infectious diseases, Harlem Medical Center, and Columbia university, NY 10027, USA Hajihosb@nychhc.org

E. B. Klerman is with the Department of Neurology at Massachusetts General Hospital Boston, MA 02114 USA and Harvard Medical School, Boston, MA 02115 USA. ebklerman@hms.harvard.edu and migratory rate of cellular active matter to promote wound healing; they act in mostly autocrine (signaling the cell that produced it) or paracrine (signaling the cells in the vicinity of the cell that produced it) fashion [3]. In the case of a systemic threat such as infection or surgery, a commensurate systemic (i.e., whole-body) inflammatory response is invoked. This involves the localized and systemic production of cytokines which then circulate in the blood (similar to hormone circulation) and stimulate the hormones in the hypothalamus-pituitary-adrenal (HPA) axis resulting in the production of corticotropin releasing hormone (CRH) in the hypothalamus, then adrenocorticotropic hormone (ACTH), an anterior pituitary hormone, and finally cortisol from the adrenal glands [1]. ACTH and cortisol promote protective inflammatory response [1], [4], [5].

Cytokines exhibit pleiotropy (i.e., a single cytokine may have more than one function) and redundancy (i.e., many cytokines can share function), as part of a robust inflammatory response [6]. The immune response elicited during bodily threats is still specific to the nature of the threat. This specificity is produced by the signaling mechanism as well as the relative abundance of each cytokine in the vicinity of the injury or threat [1]. The cytokines are capable of binding to the receptors in the target to enhance the target cell's functionalities ("normal signaling"), while trans-signaling enables the modulation of the target cells' ability to bind to other cytokines [2]. Through stimulation of the hormones of the HPA axis, cytokines mediate the acute phase response that involves fever, anorexia, production of specialized proteins and changes in plasma cation concentrations. A balance between the cytokines and regulating hormones is necessary to ensure that the immune response is appropriate [1].

In the presence of an adverse stimulus, cytokines are produced in larger quantities - up to a thousand-fold more and may cause health complications [4], [5]. For example, patients with auto-immune disorders are most likely to have post-pericardiotomy syndrome after undergoing cardiac surgery [7], [8]. Recent work has revealed the role played by cytokine storm in patients after infection with severe acute respiratory syndrome coronavirus 2 (SARS-CoV-2) [9], [10]. In both cases, the patient prognosis is crucially dependent on whether or not there is a dysregulated inflammatory response. Despite the extensive research on the versatile nature of cytokine actions in mediating the bodily inflammatory response, the dearth of high resolution longitudinal data under many disease conditions means that little is known on the temporal and causal interactions between the

different cytokines and between the cytokines and cortisol. For instance, some studies on the inflammatory response during cardiac surgery include fewer than ten measurements over a 24-hour period [11]; such infrequent sampling creates a loss of crucial information on the temporal evolution of the inflammatory response [12]. Given the many harmful side effects of an abnormal inflammatory response such as organ failure, sepsis, shock and potentially death, it is crucial to understand their dynamics to enable early detection and mitigation of adverse outcomes including prolonged hospitalization [13]. Therefore, in this work we seek to quantify cytokine and cortisol responses to cardiac surgery using mathematical models.

II. INFLAMMATION RESPONSE DURING CORONARY ARTERIAL BYPASS GRAFTING

Coronary arterial bypass grafting (CABG) surgery is a procedure performed to remedy arterial blockage. During surgery, the inflammatory response is initiated by many surgical factors including tissue injury, the interaction of tissues and blood with extracorporeal mechanical devices, ischemia and reperfusion injury invoking a systemic inflammatory response. Four cytokines - interleukins (IL) 6, 8, 10 and tumor necrosis factor (TNF) α - have been noted for their correlation with patient prognosis and duration of hospitalization in surgery [14], [15]. Of these, IL6, IL8 and TNF α are proinflammatory and interact to enhance each others' functions, while IL10 is an anti-inflammatory cytokine capable of autoregulation as well as downregulation of the proinflammatory cytokines. We consider the time evolution of these four cytokines together with cortisol which plays an important role in downregulating the inflammatory response [16], to identify their pulsatile signaling and perform causality analysis.

A. Dataset

The dataset of cytokines and cortisol levels is from the original, previously published clinical study of ten patients undergoing CABG surgery from [4]. Ten male patients (ages 57-75 years, averaging 65 ± 6.2 years) underwent elective surgery with median sternotomy with or without cardiopulmonary bypass (5 each). For all the patients, surgery was scheduled at 08:00 AM and their inflammatory marker levels were sampled every ten minutes with the first sample for all patients in the time window 8:15 AM - 9:10 AM via insitu vascular catheters for twelve hours. The data comprised several markers of inflammation including serum levels of ACTH, cortisol, and cytokines such as interleukins (IL1 α , IL2, IL4, IL6, IL8, IL10) and TNF α . For more details on the experiment and data collection including the chemical assay analysis procedures, we refer the reader to [4]. This dataset did not include data from healthy control subjects.

III. MODEL

System-theoretic modeling of complex physiological processes offer a tractable solution for identifying the macroscopic dynamics of these processes [17], [18]. Such models

have been used to understand the dynamics of neuroendocrine hormones (including cortisol [19]–[22], leptin [23] and growth hormone [24], [25]) and electrodermal activity [26]–[29]. We take a similar approach to modeling cytokine dynamics and propose second order system-theoretic model to capture the kinetics of each cytokine separately. At this stage, we assume that the cytokines are produced independently of each other, and stimulated by a single stimulus, combining the influence of all surgical factors including anesthesia, and anti-inflammatory treatment. Rather than including explicit interactions between cytokines, we choose to perform deconvolution to recover all the underlying secretory pulses that result in the observed cytokine dynamics, which is presumably a culmination of the localized inflammation due to tissue injury, systemic inflammatory response through cascaded feedback interactions between each of them, and the influence of aforementioned surgical factors. The goal of this model-based analysis is two-fold: (i) characterization of the cytokine expression through identification of underlying secretory events as a marked point process and (ii) determination of a model-based physiologically plausible smoothed cytokine data as a continuous function of time, allowing for causality analysis. These are important first steps for analyzing the inflammatory response of cytokines in relation to each other, and to ensure that the effect of measurement noise is mitigated in analysis, as is often the practice in generative model-based smoothing [30]. The dynamics of each cytokine can be written as

$$\dot{x}_1(t) = -\zeta_I x_1(t) + u(t) \tag{1}$$

$$\dot{x}_2(t) = \zeta_I x_1(t) - \zeta_C x_2(t) \tag{2}$$

where $x_1(t)$ is the cytokine produced locally at the site of inflammation, $x_2(t)$ is the measured serum cytokine level, $u(t) = \sum_{i=1}^N q_i \delta(t-\tau_i)$ is the train of secretory pulses that result in cytokine production, with q_i , τ_i and N denoting respectively the amplitude, timing and total possible number of discrete stimulatory events. Here, N=720 for the recovery of underlying stimulatory events with over the 12-hour duration. ζ_I and ζ_C refer to the rates of infusion and clearance of cytokine in the plasma. The measurements obtained every ten minutes are given by

$$y(t_i) = x_2(t_i) + \eta_{t_i} (3)$$

where the sampled serum contains the time-varying cytokine level and is subject to a measurement noise $\eta(t_i)$. We assume that the measurement noise at each instant is an independent, Gaussian distributed random variable. Note that in our model, we do not explicitly account for a basal cytokine production. We solve the system of equations (1) and (2) to obtain the measurements every ten minutes, by taking into account the effect of initial cytokine levels and the series of secretory stimuli. Denoting the system matrices

$$A = \begin{bmatrix} -\zeta_I & 0 \\ \zeta_I & -\zeta_C \end{bmatrix}, B = \begin{bmatrix} 1 \\ 0 \end{bmatrix}, C = \begin{bmatrix} 0 & 1 \end{bmatrix}$$
 (4)

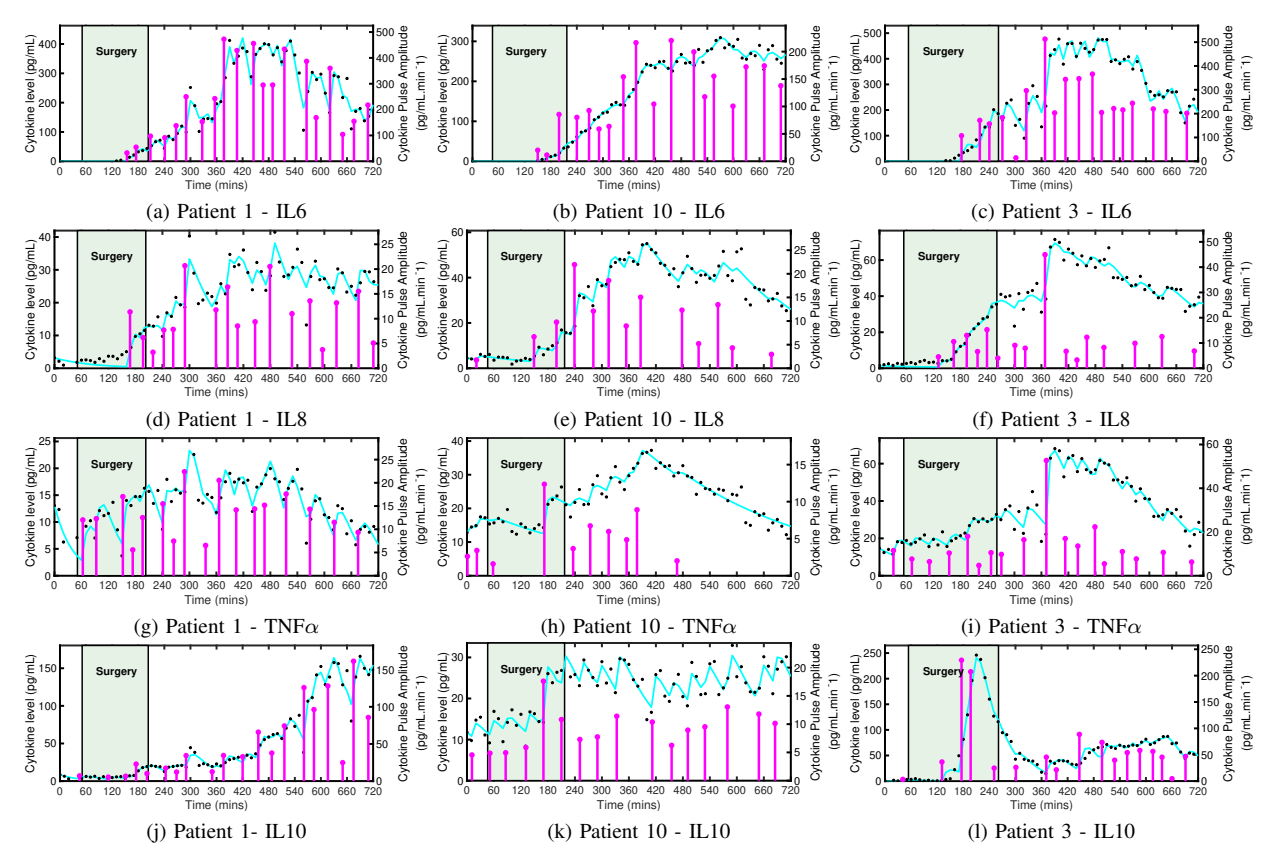


Fig. 1: Cytokine deconvolution results for patient 1, 10 and 3 for proinflammatory cytokines (IL6, IL8, TNF α) and antiinflammatory cytokine (IL10) for 720 minutes starting from first sample times ranging between 8:15 AM - 9:10 AM. Figure depicts the cytokine levels measured every ten minutes (black *), cytokine levels reconstructed every minute using our analysis (blue line) and the estimated underlying secretory pulses (pink bars). The duration of surgery is annotated in green.

and denoting the one minute sampling interval T_u , we can write

$$x(t_{k+1}) = \Lambda x(t_k) + \Gamma u(t_k) \tag{5}$$

 $\Lambda = \exp{(AT_u)}, \Gamma = \int_0^{T_u} \exp{(A(T_u - \sigma))} B d\sigma$, where $u(t) = \sum_{i=1}^N q_i \delta(t - \tau_i)$ with the measurement being

$$y(t_k) = Cx(t_k) + \eta(t_k) \tag{6}$$

Therefore, commensurate with the frequency of blood sampling, the measurement intervals $T_y = LT_u$, where L = 10. Letting $A_d = \Lambda^L$, $B_d = [\Lambda^{L-1}\Gamma \ \Lambda^{L-2}\Gamma \ ... \ \Gamma]$, $u_d[k] = [u[Lk] \ u[Lk+1] \ ... \ u[Lk+L-1]]^T$, $\eta_d[k] = \eta[Lk]$, the multi-rate system can be written as

$$x_d[k+1] = A_d x_d[k] + B_d u_d[k]$$
 (7)

$$y[k] = Cx_d[k] + \eta_d[k] \tag{8}$$

Finally, we write the measurement equations at each discrete measurement instant given by

$$y[k] = F[k]x_d[0] + D[k]u + \eta_d[k]$$
(9)

where $F[k] = CA_d^k$, $D[k] = C[A_d^{k-1}B_d \ A_d^{k-2}B_d \ \dots \ B_d \ 0 \ \dots \ 0]$ (with the last N-kL entries being zero due to causality),

 $u = [u_d[0] \ u_d[1] \ ... \ u_d[M-1]]^T$. Letting $X_d[0] = [0 \ y_{t_0}]^T$, and concatenating the outputs and the matrices, we get $\mathbf{y} = [y[0] \ ... y[M-1]]^T$, $\mathbf{F}_\zeta = [F[0] \ F[1] \ ... \ F[M-1]]^T$, $\mathbf{D}_\zeta = [D[0] \ ... \ D[M-1]]^T$, and the measurement noise $\eta = [\eta[1] \ ... \ \eta[M]]^T$, so that the measurements are given by

$$\mathbf{y} = \mathbf{F}_{\mathcal{L}} X_d[0] + \mathbf{D}_{\mathcal{L}} \mathbf{u} + \eta \tag{10}$$

A. Deconvolution

We perform deconvolution to quantify the timing and amplitude of the underlying secretory pulses and reconstruct the cytokine data at a one-minute time resolution by formulating a least squares optimization problem that seeks to minimize the cost based on the previously published algorithm [24]:

$$J_{\lambda}(\zeta, \mathbf{u}) = \frac{1}{2} ||\mathbf{y} - \mathbf{F}_{\zeta} X_d[0] - \mathbf{D}_{\zeta} \mathbf{u}||_2^2 + \lambda ||u||_p^p$$
 (11)

subject to:
$$\mathbf{C}\zeta \le \mathbf{b}, \ \mathbf{u} \ge 0, \ 0 \le ||\mathbf{u}||_0 \le 20$$
 (12)

where λ is a regularization parameter and p=0.5 is chosen to enforce the sparsity constraint. We have imposed three constraints based on earlier work [20] to ensure biological plausibility of the solution. The first, $\mathbf{C}\zeta \leq \mathbf{b}$, with

$$\mathbf{C} = \begin{bmatrix} -1 & -1 & 0 \\ 1 & 0 & -1 \end{bmatrix}^T, \ \mathbf{b} = [0 \ 0 \ 0]^T$$
 (13)

TABLE I: Infusion rate (ζ_I, \min^{-1}) , clearance rate (ζ_C, \min^{-1}) , number of secretory pulses $(||\mathbf{u}||_0)$ underlying the cytokine production, and multiple correlation coefficients (R^2) of the fit for IL6 and IL8.

Sub	ζ_I	ζ_C	$ \mathbf{u} _0$	R^2	ζ_I	ζ_C	$ \mathbf{u} _0$	R^2
No.	(IL6)	(IL6)	(IL6)	(IL6)	(IL8)	(IL8)	(IL8)	(IL8)
1	0.10	0.04	20	0.98	0.32	0.01	17	0.95
2	0.14	0.01	18	0.99	0.16	0.008	17	0.98
3	0.10	0.02	18	0.99	0.12	0.06	16	0.98
4	0.19	0.007	18	0.99	0.18	0.003	11	0.98
5	0.23	0.01	19	0.98	0.10	0.02	14	0.96
6	0.02	0.016	13	0.99	0.27	0.003	9	0.94
7	0.16	0.007	16	0.99	0.31	0.003	13	0.95
8	0.16	0.01	18	0.99	0.03	0.005	11	0.93
9	0.23	0.03	19	0.95	0.25	0.01	17	0.90
10	0.03	0.016	18	0.99	0.25	0.005	13	0.97
Median	0.15	0.014	18	0.99	0.22	0.006	13.5	0.95
Std. Dev.	0.07	0.01	1.9	0.02	0.10	0.004	2.9	0.03

TABLE II: Infusion rate (ζ_I, \min^{-1}) , clearance rate (ζ_C, \min^{-1}) , number of secretory pulses $(||\mathbf{u}||_0)$ underlying the cytokine production, and multiple correlation coefficients (R^2) of the fit for TNF α and IL10.

Sub No.	ζ_I (TNF α)	ζ_C (TNF α)	$ \mathbf{u} _0$ (TNF α)	R^2 (TNF α)	ζ_I (IL10)	ζ_C (IL10)	u ₀ (IL10)	(IL10)
1101					/		<u> </u>	
1	0.10	0.03	17	0.84	0.08	0.02	20	0.99
2	0.09	0.02	18	0.98	0.06	0.02	16	0.98
3	0.16	0.01	18	0.96	0.08	0.02	17	0.98
4	0.06	0.008	12	0.90	0.13	0.013	12	0.97
5	0.05	0.014	13	0.97	0.04	0.03	13	0.99
6	0.10	0.004	7	0.89	0.16	0.02	10	0.98
7	0.18	0.002	7	0.85	0.08	0.03	20	0.98
8	0.10	0.002	7	0.93	0.07	0.01	13	0.99
9	0.32	0.014	18	0.86	0.11	0.05	19	0.99
10	0.22	0.003	10	0.92	0.27	0.008	16	0.90
Median	0.10	0.01	12.5	0.91	0.08	0.02	16	0.98
Std. Dev.	0.08	0.008	4.80	0.05	0.07	0.01	3.5	0.03

ensures that the infusion rate is greater than the clearance rate and both the parameters are positive. Additional constraints on the pulse train ${\bf u}$ ensures that the recovered pulses are nonnegative and their total number does not exceed 20 over the 12 hour duration to balance fidelity of fit to the measurement data and sparsity (20 secretory events over 720 minutes). We use a coordinate descent approach to find the minimum cost for a prescribed value of λ using the discrete update equations:

$$\mathbf{u}^{(k+1)} = \operatorname{argmin} \ J_{\lambda}(\zeta^{k}, \mathbf{u}^{(k)})$$
subject to: $\mathbf{C}\zeta \leq \mathbf{b}, \mathbf{u} \geq 0, 0 \leq ||\mathbf{u}||_{0} \leq 20$

$$\zeta^{(k+1)} = \operatorname{argmin} \ J_{\lambda}(\zeta^{k}, \mathbf{u}^{k+1})$$
(15)

The rate parameters for each cytokine were initialized by first sampling a uniform random variable w in the interval $[8.3\times 10^{-4},\ 1]$ and then setting $\zeta=[w\ w/4]$. We perform a spline interpolation to determine the value of any missing data points in the original dataset. Then, the non-convex optimization problem [31] is solved stage-wise to determine the rate parameters and the underlying pulses: initially the FOCUSS+ algorithm is used to obtain optimized ${\bf u}$ and ζ values using the following update equations [32]. Letting $\lambda_{max}=0.1$, for r=1,2,...,30:

1.
$$\begin{aligned} & \mathbf{P}_{\mathbf{u}}^{(r)} = \operatorname{diag}(||\mathbf{u}_{i}^{(r)}|^{2-p}) \\ & 2. \ \ \lambda^{(r)} = \left(1 - \frac{||\mathbf{y}_{\zeta} - \mathbf{D}_{\zeta}\mathbf{u}^{(r)}||_{2}}{||\mathbf{y}_{\zeta}||_{2}}\right) \lambda_{max}, \ \lambda^{(r)} > 0 \\ & 3. \ \ \mathbf{u}^{(r+1)} = \mathbf{P}_{\mathbf{u}}^{(r)} \mathbf{D}_{\zeta}^{T} \left(\mathbf{D}_{\zeta}\mathbf{P}_{\mathbf{u}}^{(r)} \mathbf{D}_{\zeta}^{T} + \lambda^{(r)} \mathbf{I}\right)^{-1} (\mathbf{y} - \mathbf{F}_{\zeta}X_{d}[0]) \\ & 4. \ \ \mathbf{u}_{i}^{(r+1)} \leq 0 \ \ \rightarrow \ \mathbf{u}_{i}^{(r+1)} = 0 \end{aligned}$$

- 5. After completing more than half of the total iterations, if $||\mathbf{u}^{(r+1)}||_0 > 20$, select the largest 20 values from $\mathbf{u}^{(r+1)}$ and set the rest to zero
- 6. Update ζ using equation (15)
- 7. Iterate

In the second stage, the generalized cross validation [33] together with FOCUSS+ is used to obtain the final solution, where the initial pulses and rate parameters are set to the value obtained from the solution to the first stage of FOCUSS+ algorithm and the regularization parameter is updated as the solution to minimizing the following term:

$$G(\lambda) = \frac{N_d(\mathbf{I} - \mathbf{H}_{\lambda})\mathbf{y}_{\zeta}}{(trace(\mathbf{I} - \mathbf{H}_{\lambda}))^2}$$
(16)

Here, N_d is the number of data points, and \mathbf{H}_{λ} is the influence matrix, which in our algorithm is

$$\mathbf{H}_{\lambda} = \mathbf{D}_{\zeta} \mathbf{P}_{\mathbf{u}}^{(r)} \mathbf{D}_{\zeta}^{T} \left(\mathbf{D}_{\zeta} \mathbf{P}_{\mathbf{u}}^{(r)} \mathbf{D}_{\zeta}^{T} + \lambda^{(r)} \mathbf{I} \right)^{-1}$$
(17)

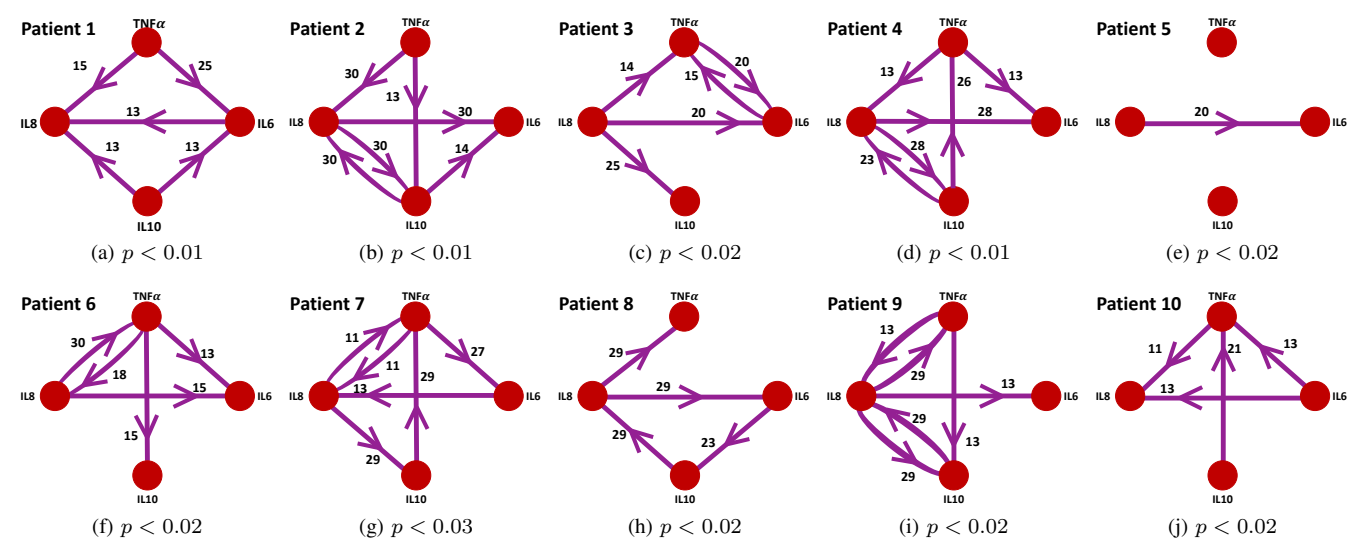


Fig. 2: Granger causality analysis of deconvolved cytokines is depicted for each patient. The four red nodes (from top node, clockwise) refer to the cytokines TNF α , IL6, IL10 and IL8. The directed graph shows the directionality of the statistically significant causal relationships using the edge arrows and the optimal lag parameters are indicated as edge weights. The range of significance values are indicated in subtitles for each patient.

This step is run for 200 iterations and the optimal set of pulses and infusion and clearance rate parameters are obtained based on the cost criterion. A more detailed discussion of this algorithm can be found in [24]. To numerically stabilize this algorithm, we first re-scaled the cytokine levels, dividing them by 10. We then transformed the cytokine levels back to the original units after performing deconvolution analysis to recover the underlying secretory events.

B. Granger causality analysis between cytokines

After performing deconvolution to obtain estimates of both the cytokine levels and the underlying secretory pulses at a one-minute sampling rate, we perform Granger causality test [34] between all possible pairs of cytokines to determine dyadic causal interactions between them. Since any interactions between the cytokines and feedback loops involving the HPA axis are captured by means of the secretory stimuli ${\bf u}$ and we do not explicitly model any interactions between the cytokines, we perform pairwise tests to uncover patient-specific relationships. For two signals of types A and B whose measurements are given by y_A and y_B , we test the validity of a causal model of the form:

$$y_A(t_k) = \sum_{j=1}^{N_{A,A}} \alpha_{A,j} y_A(t_k - j) + \sum_{j=1}^{N_{A,B}} \beta_{A,j} y_B(t_k - j) + \epsilon(t_k)$$
(18)

Here, the signal y_A at time instant t_k is represented as a linear combination of two components: the past values of the same signal denoted as $\{y_A(t_k-j)\}_{j=1}^{N_{A,A}}$, and the past values of y_B denoted as $\{y_B(t_k-j)\}_{j=1}^{N_{A,B}}$, where $N_{A,A}$ and $N_{A,B}$ are the number of terms of the respective signal history that are used to test the causality, and $\epsilon(t_k)$ represents an error term. We use the MATLAB function gctest [35] to perform

this causality test. If the signals can be represented with at least one of the coefficients $\beta_{A,j}$ non-zero with statistical significance, then we say that y_B causes y_A . We set the range of $N_{A,A}$ and $N_{A,B}$ to be a maximum of 30 minutes and construct a linear model of the form 18 to fit the data. Then, we use the minimization of the Akaike Information Criterion (AIC) to calculate the optimal lag parameter.

IV. RESULTS AND DISCUSSION

We performed the deconvolution analysis to quantify the timing and amplitude of the underlying secretory pulses stimulating the production of all four cytokines for all ten patients. The algorithm recovered the cytokine levels with high fidelity: of the total 40 deconvolutions performed, all but five had multiple correlation coefficients greater than 0.9, with the lowest being 0.84. The recovered infusion and clearance rate parameters, and total number of pulses recovered are listed in Table I and II. We show three representative results in Fig. 1 based on three subject classifications based on the HPA axis response in [5], since this was used to predict subjects with the greatest inflammatory response in their work.

The cytokine levels and the underlying secretory pulses are plotted for three patients in Fig. 1; for these patients, the cytokine levels significantly increased post-surgery. For patient 3 in Fig. 1 (1), IL10 peaked during surgery and diminished in the hours thereafter, earlier than other cytokines for this and other patients. The patterns of pulse amplitudes varied across all patients and all cytokines. IL6 and IL10 had had a median of 18 and 16 secretory pulses underlying their production across all ten patients respectively, while IL8 and $TNF\alpha$ had medians of 13.5 and 12.5 (Table I, II). The infusion rates of IL6 and IL8 showed higher medians,

while the median values of rate of infusion of TNF α and IL10 were comparatively less. The median clearance rates showed considerable variability for all four cytokines. The standard deviations of the metrics (Table I, II) were similar for all cytokines; relative to the median value, these values showed larger variability, though. Despite the variability in the recovered secretory events, we observe that for patient 3, the largest amplitude secretory event for IL6, IL8 and TNF α occurs post-surgery at around 360 minutes, and is followed by a smaller secretory response from IL10. The largest amplitude secretory event for IL10 for this patient at 180 minutes occurs during surgery and is accompanied by smaller secretory events in the proinflammatory cytokines. For patient 1, concomitant large amplitude pulses were observed just before 300 minutes for the proinflammatory cytokines, corresponding to peaking TNF α , together with a corresponding secretory event for IL10. For patient 10, such co-occurring pulses were not prominently seen for proinflammatory cytokines but IL8 and IL10 showed such a pulse during surgery shortly before 180 minutes.

The co-occurrence of cytokine response events may shed light on the intricate feedback mechanisms involved in modulating the immune response. We summarize these relationships using the results of the dyadic Granger causality analysis between the cytokines are shown in Figure 2. Crucially, all patients showed a causal relationship between IL6 and IL8, seven patients between IL6 and TNF α , six patients between IL6 and IL10, seven patients between IL8 and IL10, nine patients between IL8 and TNF α , and six patients between TNF α and IL10; some of these interactions are hypothesized in literature [1], [2]. We note that the directionality of these causal relationships are not uniform across all the patients. For example, seven patients had IL8 causing IL6, while others had the directionality of this relationship reversed. Bidirectional relationships recovered in some subjects between IL8 and IL10 in three patients, IL8 and TNF α in three patients and IL6 and TNF α in one patient indicate the possible existence of feedback relationships in these patients [34]. Note that in this analysis, we only test whether the null hypothesis that the coefficients $\beta_{A,j}$ are all zero can be rejected or not. In future work, we will expand this and explore the exact nature of this causality relationship, to distinguish stimulatory and inhibitory feedback signaling [27]. Although we have identified models for each individual cytokine secretory process, we have not delineated the differences between an individual cytokine expression based on the stimulatory effect of other cytokines or the influence exogenous factors such as anesthesia and medication through an increase in the anti-inflammatory action. Therefore, in addition to the causality analysis based on the cytokine levels, we plan to determine the causality of the underlying secretory events [36] and infer models for cytokine interactions in future work. We expect that more data on the surgical factors will help refine these models for the complex cytokine response.

V. CONCLUSIONS AND FUTURE WORK

In this research, we have investigated the response of cytokines and have performed deconvolution to estimate the rate parameters governing their production and clearance in individuals who are undergoing cardiac surgery. The recovered pulses and the reconstructed cytokine levels indicate statistically significant dyadic interactions, although they were not present uniformly across all patients. Note that (i) our model structure means that we only observe the overall effect of the complex feedback interactions between cytokines and hormones. Therefore, we expect that a more mechanistic model that explicitly accounts for feedback interactions will help explain these observations. (ii) Some relationships had lag terms nearly equal to the maximum specified value; these relationships must be investigated with different maximum limits on the lag parameter in future work. In future work, we intend to investigate the models that incorporate hypothesized positive and negative feedback interactions between IL6, IL8, IL10, TNF α , together with ACTH and cortisol, and perform concurrent deconvolution to infer the state of inflammation of patients. Extension of the causality analysis to include multilateral interactions between the inflammatory markers will also help test the validity of hierarchical models hypothesized for cytokine production during surgery. This line of work could eventually help in informing medical interventions to ensure a controlled inflammatory response, thereby improving medical outcomes for patients suffering from many conditions.

REFERENCES

- A. V. Turnbull and C. L. Rivier, "Regulation of the hypothalamicpituitary-adrenal axis by cytokines: actions and mechanisms of action," *Physiological reviews*, 1999.
- [2] A. W. Thomson and M. T. Lotze, The Cytokine Handbook, Two-Volume Set. Elsevier, 2003.
- [3] T. J. Fahey III, B. Sherry, K. J. Tracey, S. van Deventer, W. G. Jones II, J. P. Minei, S. Morgello, G. T. Shires, and A. Cerami, "Cytokine production in a model of wound healing: the appearance of mip-1, mip-2, cachectin/tnf and il-i," *Cytokine*, vol. 2, no. 2, pp. 92–99, 1990.
- [4] D. Galvis, E. Zavala, J. J. Walker, T. Upton, S. L. Lightman, G. D. Angelini, J. Evans, C. A. Rogers, K. Phillips, and B. Gibbison, "Modelling the dynamic interaction of systemic inflammation and the hypothalamic–pituitary–adrenal (hpa) axis during and after cardiac surgery," *Journal of the Royal Society Interface*, vol. 19, no. 189, p. 20210925, 2022.
- [5] B. Gibbison, D. M. Keenan, F. Roelfsema, J. Evans, K. Phillips, C. A. Rogers, G. D. Angelini, and S. L. Lightman, "Dynamic pituitary–adrenal interactions in the critically ill after cardiac surgery," *The Journal of Clinical Endocrinology & Metabolism*, vol. 105, no. 5, pp. 1327–1342, 2020.
- [6] K. Ozaki and W. J. Leonard, "Cytokine and cytokine receptor pleiotropy and redundancy," *Journal of Biological Chemistry*, vol. 277, no. 33, pp. 29355–29358, 2002.
- [7] F. Maranta, L. Cianfanelli, R. Grippo, O. Alfieri, D. Cianflone, and M. Imazio, "Post-pericardiotomy syndrome: insights into neglected postoperative issues," *European Journal of Cardio-Thoracic Surgery*, vol. 61, no. 3, pp. 505–514, 2022.
- [8] B. K. Tamarappoo and A. L. Klein, "Post-pericardiotomy syndrome," Current cardiology reports, vol. 18, pp. 1–5, 2016.
- [9] D. C. Fajgenbaum and C. H. June, "Cytokine storm," New England Journal of Medicine, vol. 383, no. 23, pp. 2255–2273, 2020.
- [10] B. Hu, S. Huang, and L. Yin, "The cytokine storm and covid-19," Journal of medical virology, vol. 93, no. 1, pp. 250–256, 2021.

- [11] S. Wan, A. Marchant, J.-M. DeSmet, M. Antoine, H. Zhang, J.-L. Vachiery, M. Goldman, J.-L. Vincent, and J.-L. LeClerc, "Human cytokine responses to cardiac transplantation and coronary artery bypass grafting," *The Journal of Thoracic and Cardiovascular Surgery*, vol. 111, no. 2, pp. 469–477, 1996.
- [12] B. Powell, G. P. Nason, G. D. Angelini, S. L. Lightman, and B. Gibbison, "Optimal sampling frequency of serum cortisol concentrations after cardiac surgery," *Critical care medicine*, vol. 45, no. 10, pp. e1103–e1104, 2017.
- [13] G. Cappabianca, C. Rotunno, L. d. L. T. Schinosa, V. M. Ranieri, and D. Paparella, "Protective effects of steroids in cardiac surgery: a metaanalysis of randomized double-blind trials," *Journal of cardiothoracic* and vascular anesthesia, vol. 25, no. 1, pp. 156–165, 2011.
- [14] J. McGuinness, D. Bouchier-Hayes, and J. Redmond, "Understanding the inflammatory response to cardiac surgery," *The Surgeon*, vol. 6, no. 3, pp. 162–171, 2008.
- [15] V. Brix-Christensen, E. Tønnesen, I. Sørensen, T. Bilfinger, R. Sanchez, and G. Stefano, "Effects of anaesthesia based on high versus low doses of opioids on the cytokine and acute-phase protein responses in patients undergoing cardiac surgery," *Acta anaesthesio-logica scandinavica*, vol. 42, no. 1, pp. 63–70, 1998.
- [16] M. P. Fillinger, A. J. Rassias, P. M. Guyre, J. H. Sanders, M. Beach, J. Pahl, R. B. Watson, P. K. Whalen, K.-T. J. Yeo, and M. P. Yeager, "Glucocorticoid effects on the inflammatory and clinical responses to cardiac surgery," *Journal of cardiothoracic and vascular anesthesia*, vol. 16, no. 2, pp. 163–169, 2002.
- [17] R. T. Faghih, K. Savla, M. A. Dahleh, and E. N. Brown, "A feedback control model for cortisol secretion," in 2011 Annual International Conference of the IEEE Engineering in Medicine and Biology Society, pp. 716–719, IEEE, 2011.
- [18] R. T. Faghih, "From physiological signals to pulsatile dynamics: a sparse system identification approach," in *Dynamic Neuroscience*, pp. 239–265, Springer, 2018.
- [19] D. D. Pednekar, M. R. Amin, H. F. Azgomi, K. Aschbacher, L. J. Crofford, and R. T. Faghih, "Characterization of cortisol dysregulation in fibromyalgia and chronic fatigue syndromes: a state-space approach," *IEEE Transactions on Biomedical Engineering*, vol. 67, no. 11, pp. 3163–3172, 2020.
- [20] D. D. Pednekar, M. R. Amin, H. F. Azgomi, K. Aschbacher, L. J. Crofford, and R. T. Faghih, "A system theoretic investigation of cortisol dysregulation in fibromyalgia patients with chronic fatigue," in 2019 41st Annual International Conference of the IEEE Engineering in Medicine and Biology Society (EMBC), pp. 6896–6901, IEEE, 2019.
- [21] A. Yaghmour, M. R. Amin, and R. T. Faghih, "Decoding a music-modulated cognitive arousal state using electrodermal activity and functional near-infrared spectroscopy measurements," in 2021 43rd Annual International Conference of the IEEE Engineering in Medicine & Biology Society (EMBC), pp. 1055–1060, IEEE, 2021.
- [22] R. T. Faghih, P. A. Stokes, M.-F. Marin, R. G. Zsido, S. Zorowitz, B. L. Rosenbaum, H. Song, M. R. Milad, D. D. Dougherty, E. N. Eskandar, et al., "Characterization of fear conditioning and fear extinction by

- analysis of electrodermal activity," in 2015 37th Annual International Conference of the IEEE Engineering in Medicine and Biology Society (EMBC), pp. 7814–7818, IEEE, 2015.
- [23] M. R. Amin, D. D. Pednekar, H. F. Azgomi, H. Van Wietmarschen, K. Aschbacher, and R. T. Faghih, "Sparse system identification of leptin dynamics in women with obesity," *Frontiers in endocrinology*, vol. 13, 2022.
- [24] J. X. Genty, M. R. Amin, N. D. Shaw, E. B. Klerman, and R. T. Faghih, "Sparse deconvolution of pulsatile growth hormone secretion in adolescents," *IEEE/ACM Transactions on Computational Biology and Bioinformatics*, vol. 19, no. 4, pp. 2463–2470, 2021.
- [25] M. E. Calvert, S. A. Molsberry, T. Kangarloo, M. R. Amin, V. Genty, R. T. Faghih, E. B. Klerman, and N. D. Shaw, "Acute sleep disruption does not diminish pulsatile growth hormone secretion in pubertal children," *Journal of the Endocrine Society*, 2022.
- [26] M. R. Amin and R. T. Faghih, "Inferring autonomic nervous system stimulation from hand and foot skin conductance measurements," in 2018 52nd Asilomar Conference on Signals, Systems, and Computers, pp. 655–660, IEEE, 2018.
- [27] M. R. Amin and R. T. Faghih, "Sparse deconvolution of electrodermal activity via continuous-time system identification," *IEEE Transactions* on *Biomedical Engineering*, vol. 66, no. 9, pp. 2585–2595, 2019.
- [28] M. R. Amin and R. T. Faghih, "Robust inference of autonomic nervous system activation using skin conductance measurements: A multichannel sparse system identification approach," *IEEE Access*, vol. 7, pp. 173419–173437, 2019.
- [29] M. R. Amin and R. T. Faghih, "Tonic and phasic decomposition of skin conductance data: A generalized-cross-validation-based block coordinate descent approach," in 2019 41st Annual International Conference of the IEEE Engineering in Medicine and Biology Society (EMBC), pp. 745–749, IEEE, 2019.
- [30] B. Dey and P. Krishnaprasad, "Control-theoretic data smoothing," in 53rd IEEE Conference on Decision and Control, pp. 5064–5070, IEEE, 2014.
- [31] R. T. Faghih, M. A. Dahleh, G. K. Adler, E. B. Klerman, and E. N. Brown, "Deconvolution of serum cortisol levels by using compressed sensing," *PloS one*, vol. 9, no. 1, p. e85204, 2014.
- [32] J. F. Murray, Visual recognition, inference and coding using learned sparse overcomplete representations. University of California, San Diego, 2005.
- [33] G. H. Golub, M. Heath, and G. Wahba, "Generalized cross-validation as a method for choosing a good ridge parameter," *Technometrics*, vol. 21, no. 2, pp. 215–223, 1979.
- [34] C. W. Granger, Essays in econometrics: collected papers of Clive WJ Granger, vol. 32. Cambridge University Press, 2001.
- [35] MATLAB, version 9.12.0 (R2022a). Natick, Massachusetts: The MathWorks Inc., 2022.
- [36] A. Casile, R. T. Faghih, and E. N. Brown, "Robust point-process granger causality analysis in presence of exogenous temporal modulations and trial-by-trial variability in spike trains," *PLoS computational biology*, vol. 17, no. 1, p. e1007675, 2021.